Exp. Theo. NANOTECHNOLOGY 5 (2021) 129 – 135

Experimental and Theoretical
NANOTECHNOLOGY
http://etn.siats.co.uk/

Temperature dependence of optical study of InGaN QDs

X. Wang[1], l. Marquiz[2]

[1]Department of Physics, National University of Singapore 117576, Singapore
[2]Instituto de Nanociencia, Universidad de Zaragoza, Zaragoza, 50018, Spain
[*]E-mail: phyxw@nus.edu.sg

Received: 26/6/2020 / *Accepted:* 8/11/2020 / *Published:* 1/5/2021

Self-assembled InGaN quantum dots (QDs) were fabricated by metal-organic chemical vapor deposition. Abnormal temperature dependence of photoluminescence (PL) was observed. The integrated PL intensity of QDs sample shows a dramatic increase in a temperature range from 160 K to 215 K and reaches the maximum value at 215 K instead of 10 K as usual. To interpret this phenomenon, a theoretic model of temperature induced carrier redistribution mechanism is designed using rate equation, which fits closely with the experimental result. It is concluded that carriers' redistribution from shallow QDs or wetting layer to deep QDs gives rise to the unique behavior for InGaN QDs structure.

Keywords: CdSe; Structural; Multilayer.

1. INTRODUCTION:

InGaN based self-assembled quantum dots (QDs) via either Stranski–Krastanov (S-K) growth mode and/or phase segregation have been considered a promising approach to overcome the "green gap," which represents the rapidly declining external quantum efficiency (EQE) of nitride- based light emitting diodes (LEDs) in the green spectral region. Generally, it is believed that the deteriorated crystal quality and large piezoelectric field in InGaN alloy induced by high indium content give rise to the serious efficiency droop in green LEDs p1,2]. It is expected that self-assembled InGaN QDs could relax the strain through the formation of dot-like structure, according to the lowest energy principle [3]. Therefore, self-assembled InGaN QDs have potential to improve the luminescence efficiency of InGaN green LED with the advantages of its defect-free zero-dimension structure, hindrance of carriers' migration toward the nonradiative defects [4], and the reduced polarization effect [5].

Several groups have studied the optical property and recombination mechanism of InGaN QDs grown by metal- organic chemical vapor deposition (MOCVD) or molecular beam epitaxy (MBE) [6,7]. In this letter, InGaN QDs samples were fabricated by MOCVD through self-assembled method. An anomalous behavior in temperature dependence of photo- luminescence (PL) spectrum was observed. Differing from typical QW samples, integrated PL intensity of QDs samples do not decrease monotonically with elevated temperature but show a dramatic increase in a certain temperature range [8,9]. Similar phenomena in temperature dependent of micro-PL in- tensity for QDs in low temperature range were reported by Masumoto et al. and explained using a thermal activation model [10]. In our study, a model of carriers' redistribution in self-assembled InGaN QDs was built in form of rate equation to obtain an intensive understanding of this phenomenon.

InGaN QDs samples were grown by commercial MOCVD system. Triethylgallium (TEGa) and trimethylindium (TMIn) were used as group III source, whereas NH_3 was used as group V source. After a 25 nm thick GaN nucleation layer was deposited under 550 ^{o}C on sapphire substrate, 2 lm undoped GaN layer and 1.5 lm Si doped GaN layer were deposited sequentially under 1100 ^{o}C. Then, the temperature was reduced to 640 ^{o}C for the growth of self- assembled InGaN QDs layer. During the growth of InGaN QDs, the flow rate of TEGa, TMIn, and NH_3 was 20 sccm, 100 sccm, and 3.6 slm, respectively. The growth time of QDs layer was 60 s with the nominal thickness of 3 nm, which is estimated by the growth rate of thick InGaN film under the same condition. The uncapped InGaN QDs sample was fabricated in order to obtain a better measurement of surface morphology, while capped QDs sample was grown under the same condition except the additional GaN capping layer under 740 ^{o}C. Atomic force microscopy (AFM) scans were performed to observe the surface morphology of samples using a Nano- scope Dimension^{TM} 3100 scanning probe microscope system. A typical PL system with a He–Cd 325 nm laser was employed to perform the temperature dependent of PL measurements. The PL measurements taken for both samples were under the same condition. High resolution transmission electron microscopy (HRTEM) images were acquired with a Tecnai G2 F20 FEI-TEM microscope.

The general morphology of uncapped QDs sample is investigated by AFM shown in Fig. 1(a), which clearly indicates the feature of QDs structure with a density of 10^{11} cm^{-2}. Additionally, as seen in Fig. 1(b), the height distribution of QDs is extracted from the AFM data with a bi-modal distribution consisted of two Gaussian fits. That is, approximately there are two kinds of localized positions which are also referred to as sub-ensembles dominated in QDs layer. This observation agrees with other published

Exp. Theo. NANOTECHNOLOGY 5 (2021) 129 – 135

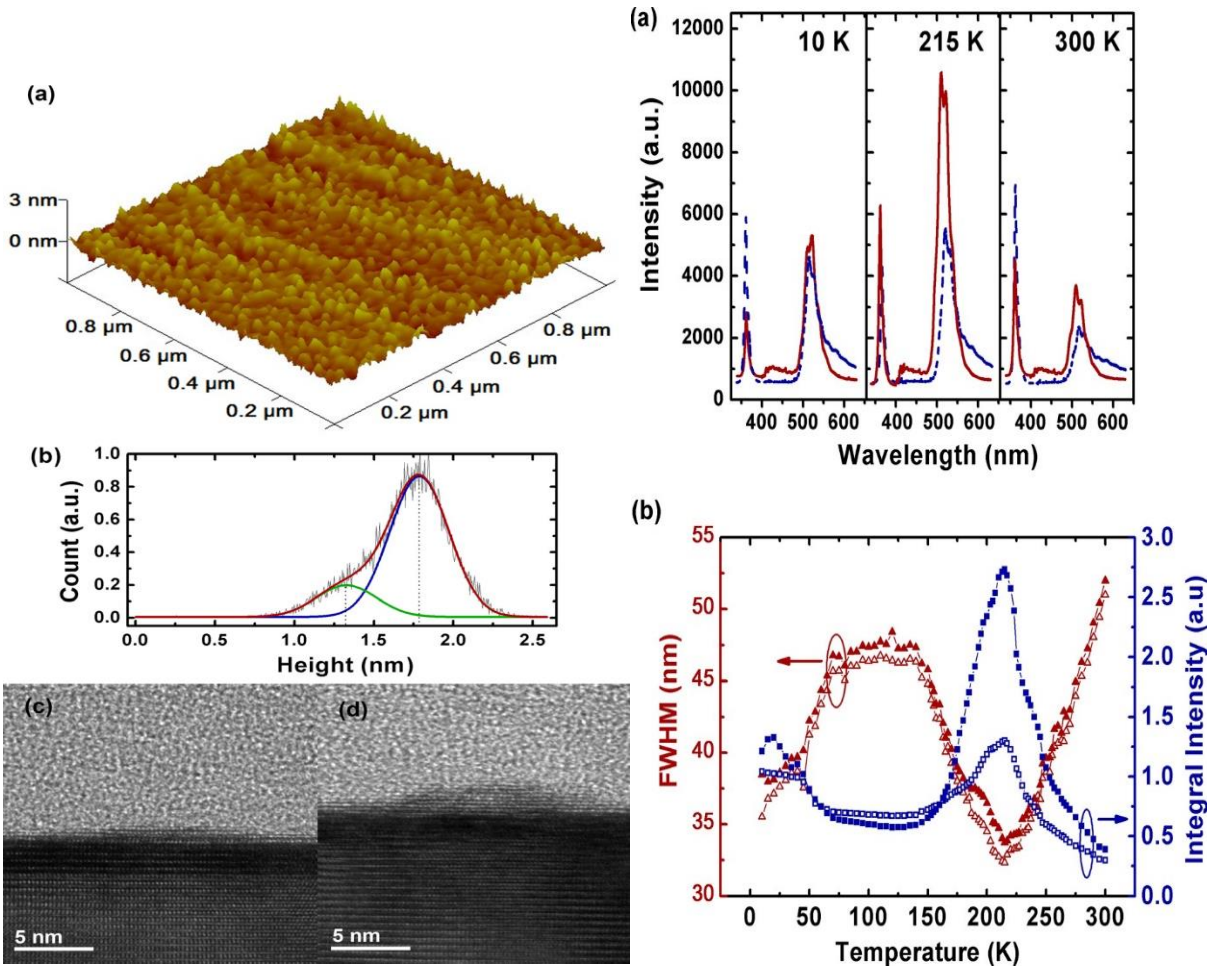

FIG. 1. (a) AFM image of uncapped QDs sample. (b) AFM height distribution for uncapped QDs sample. (c),(d) HRTEM bright field images of two isolated InGaN QDs with different height.

results of the inhomogeneous broadening of QDs ensemble property due to random variation in size and composition [9]. The evolution and physical origin of the bimodal and multi- modal distribution of QDs' height have been explicitly reported by several groups [5,6]. The detailed characteristic of QDs structure is analyzed by HRTEM. Figs. 1(c) and 1(d) show the HRTEM images of two isolated QDs structure with different size. A continuous 2D wetting layer with a thick- ness of about 2 nm was identified from both QDs structures, suggesting the SK growth mode. The heights of two QDs shown in HRTEM image are about 1 nm and 2 nm, respectively. However, the lateral widths of both QDs shown in HRTEM images are about 10 nm, which is much smaller than that measured by AFM, resulting in the aspect ratio of 0.1–0.2. The limited tip radius of AFM system may account for the discrepancy of QDs' size acquired by the AFM and HRTEM measurement. The indium incorporation obtained by energy dispersive x-ray spectroscopy (EDX) analysis is about 33% for QDs and 17% for the wetting layer, which result in the 3D confinement. Furthermore, the PL spectra for the two samples at 10 K, 215 K, and 300 K are shown in Fig. 2(a). The main emission peaks for both QDs samples are longer than 500 nm, of which the corresponding photon energies are smaller than the band edge energy of low indium wetting layer. Thus, the main emission peaks of PL spectra for

QDs samples, as seen in the Fig. 2(a), could be originated from the QDs structure. Moreover, an oscillatory structure with five peaks is visible in the PL spectra of both samples. Considering the total epilayer thickness of 3.5 lm, the consequent peaks spacing caused by Fabry-P'erot oscillation is about 15 nm in the wavelength range around 500 nm. However, the oscillatory structure peaks at 510 nm and 521 nm have the constant spacing of 11 nm over the whole temperature range. Previously, researches [7,8] have revealed that such oscillatory structure could result from the luminescence of different sub-ensembles of InGaN QDs indicated in the height distribution of QDs in Fig. 1(b). In addition, the three shoulder peaks observed in PL spectra with equal spacing of 15 nm are owing to the Fabry-P'erot oscillation.

The temperature dependence of integrated PL intensity for uncapped and capped QDs samples are shown in Fig. 2(b). The integrated PL intensities were normalized by the integrated PL intensity for capped QDs sample at 10 K to make a comprehensive comparison. It is important to notice that integrated PL intensities of both QDs samples appear to increase with temperature in the range from 160 K to 215 K and reach the maximum value at 215 K. The anomalous phenomenon implies that the recombination mechanism in QDs is different with that in QWs structures [3]. We suspect that temperature induced carriers' redistribution gives rise to this abnormal phenomenon. Another evidence is that the temperature dependence of the full width half maximum (FWHM) of PL spectrum shows an opposite behavior to the temperature dependence of integrated PL intensity, as seen in Fig. 2(b). Due to the constant energy gap between the two maxima of PL spectra over the whole temperature range, the FWHM shown in Fig. 2(b) is defined as the sum of the FWHMs for two peaks. The FWHM of PL spectrum for QDs sample becomes narrower as the integral PL intensity increases and vice versa. The variation of FWHM with temperature has also been reported by several groups as a proof of carrier redistribution in localized state assembles [9].

Considering the inhomogeneous distribution of QDs in size and composition, a simple model of InGaN QDs layer is proposed, as shown in Fig. 3. Suppose there are two kinds of sub-ensembles dominated in InGaN QDs layer correspond- ing to the peaks of two Gaussian fit in Fig. 1(b)—the shallow localized positions with localized energy of E_S and the deep localized positions with localized energy of E_D. Assume that the total excitation carriers are divided into three parts: N_W, the part of carriers in wetting layer; N_S, the part of carriers in shallow localized positions; and N_D, the part of carriers in deep localized positions. There are several mechanisms that jointly determine the carriers' density in each localized posi- tion, including photonic excitation, capture, thermal escape, and radiative and nonradiative recombination. Based on this model, the formulas that describe the carriers' redistribution mechanism were built in form of rate equation as below dependent of PL intensity for uncapped QDs sample. However, there is still discrepancy between the measured and simulated results, which may originate from the simple assumption that only two sub-ensembles were existed. In fact, the Gaussian-type height distribution of both sub-ensembles is more comprehensive. Gaussian distribution increase. Thus, it results in the decline of total radiation efficiency and the broadening of FWHM.

The simulated carrier density is plotted versus temperature, as seen in Fig. 4(b). Carrier density of shallow localized positions N_S decreases in the whole range of temperature, as a result of the thermal escape and activation of defect recombination. Then, the thermal escaped carriers can be captured by deep localized positions. When the number of carriers gained by capture was able to compensate that consumed by recombination, carriers start to accumulate and eventually lead to an enormous increase in deep localized positions. Due to the stronger confinement for carrier and better crystal quality in deep localized positions, it is reasonable to con- sider that the radiation efficiency is higher in deep localized positions. As a majority of carriers are converging into deep localized positions, the total radiation efficiency at 215 K is enhanced by a factor of 1.38 compared with that at 10 K, and the FWHM is reduced. As temperature further increases, however, more carriers escape from QDs and defect-assisted recombination is dominating. Concurrently, carriers' distribution is determined by Boltzman distribution. As a consequence of 7 nm in main emission peaks of PL spectrum for capped QDs sample compared with that for uncapped QDs sample, as seen in Fig. 2(a). As a result, oscillator strength in capped QDs weakens due to the lowered overlap between the wave- function of electron and hole by quantum confined stark effect (QCSE). Especially in QDs with larger height, the degradation of oscillator strength is more effective. The enhancement of radiative efficiency in QDs with larger height is compensated by the degeneration of oscillator strength due to the stronger QCSE. While the separation of electron and hole's wavefunction is insignificant in shallow localized QDs because of the small height. Thus, the superiority of higher radiative efficiency for the deep localized QDs compare to shallow localized QDs is diminished. That reduces the efficiency enhancement to a factor of 1.15 in the capped QDs sample, as seen in Fig. 2(b).

Exp. Theo. NANOTECHNOLOGY 5 (2021) 129 – 135

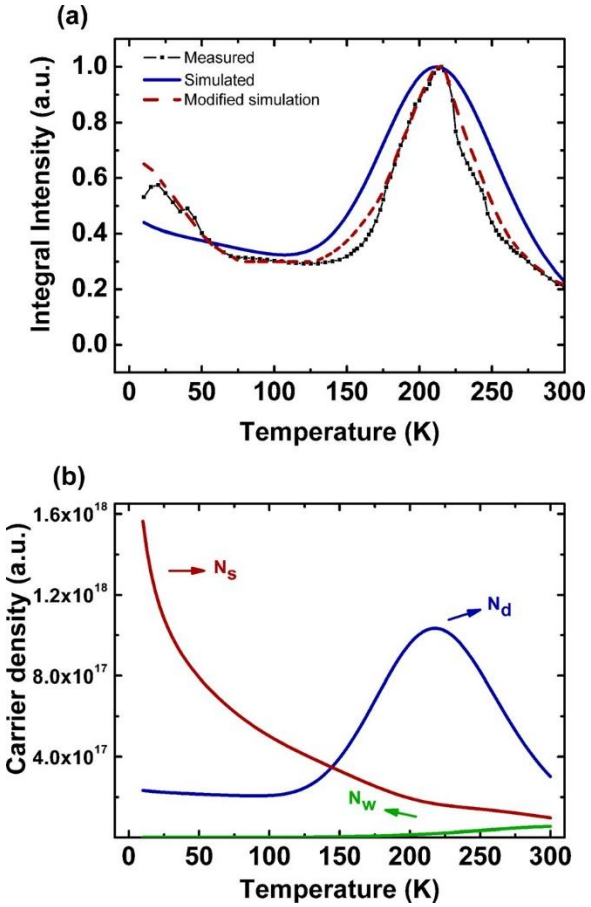

FIG. 4. (a) Simulated and measured temperature dependence of PL intensity for uncapped QDs sample. (b) Simulated N_S, N_W, N_D plotted versus temper- ature for uncapped QDs sample.

In summary, based on the analysis and simulation results of anomalous temperature dependence of integrated PL in- tensity found in uncapped and capped InGaN QDs sample, it is deduced that temperature induced carrier redistribution among different localized positions accounts for this anomalous phenomenon. Carriers' redistribution with temperature results from the competition among the escape, capture, and recombination processes. It is expected that radiation of deep localized positions is higher than that of shallow localized positions and wetting layer. Thus, in a special temperature range, when most carriers converge into deep localized positions, integrated PL intensities increase by a factor of 2.5 for uncapped QDs sample, whereas for capped InGaN QDs sample, carriers' recombination in QDs layer suffers from a stronger QCSE. That makes the efficiency enhancement diminishes to a factor of 1.25 for capped InGaN QDs layer.

Exp. Theo. NANOTECHNOLOGY 5 (2021) 129 – 135

References:

[1] D. Fuhrmann, U. Rossow, C. Netzel, H. Bremers, G. Ade, P. Hinze, and Hangleiter, Phys. Stat. Solidi C 3(6), (2006) 1966

[2] D. Fuhrmann, C. Netzel, U. Rossow, A. Hangleiter, G. Ade, and P. Hinze, Appl. Phys. Lett. 88, (2006) 071105

[3] S. Schulz and E. P. O'Reilly, Phys. Rev. B 82, (2010) 033411

[4] Liqaa H. Alwaan, Layla A. Jubur, Doaa A. Hussein, Theo. Exp. NANOTECHOLOGY 4 (2020) 35

[5] M. Zhang, A. Banerjee, C.-S. Lee, J. M. Hinckley, and P. Bhattacharya, Appl. Phys. Lett. 98, (2011) 221104

[6] T. Bartel, M. Dworzak, M. Strassburg, A. Hoffmann, A. Strittmatter, and D. Bimberg, Appl. Phys. Lett. 85, (2004) 1946

[7] J. W. Robinson, J. H. Rice, A. Jarjour, J. D. Smith, R. A. Oliver, G. A. D. Briggs, M. J. Kappers, C. J. Humphreys, and Y. Arakawa, Appl. Phys. Lett. 83, (2003) 2674

[8] Y.-H. Cho, G. H. Gainer, A. J. Fischer, J. J. Song, S. Keller, U. K. Mishra, and S. P. DenBaars, Appl. Phys. Lett. 73, (1998) 1370

[9] T. Wang, D. Nakagawa, M. Lachab, T. Sugahara, and S. Sakai, Appl. Phys. Lett. 74, (1999) 3128 [10] Y. Masumoto and T. Takagahara, Semiconductor Quantum Dot (Springer, Berlin, (2002).

Exp. Theo. NANOTECHNOLOGY 5 (2021) 129 – 135